Available online at www.sciencedirect.com
ScienceDirect
Nuclear Medicine and Biology 37 (2010) 469–477
NUCLEAR MEDICINE — AND — BIOLOGY
www.elsevier.com/locate/nucmedbio

In vivo evaluation of [^{123}I]-4-(2-(bis(4-fluorophenyl)methoxy)ethyl)-1-(4-iodobenzyl)piperidine, an iodinated SPECT tracer for imaging the P-gp transporter

Sylvie De Bruyne[a], Leonie Wyffels[a], Terrence L. Boos[b], Steven Staelens[c], Steven Deleye[c], Kenner C. Rice[b], Filip De Vos[a,*]

[a]*Laboratory for Radiopharmacy, Ghent University, 9000 Ghent, Belgium*
[b]*Chemical Biology Research Branch, National Institute on Drug Abuse and National Institute on Alcohol Abuse and Alcoholism, National Institutes of Health, Bethesda, MD, USA*
[c]*IBITECH-Medisip, Ghent University-IBBT, 9000 Ghent, Belgium*

Received 21 August 2009; received in revised form 23 October 2009; accepted 31 October 2009

Abstract

Introduction: P-glycoprotein (P-gp) is an energy-dependent transporter that contributes to the efflux of a wide range of xenobiotics at the blood–brain barrier playing a role in drug-resistance or therapy failure. In this study, we evaluated [^{123}I]-4-(2-(bis(4-fluorophenyl)methoxy)ethyl)-1-(4-iodobenzyl)piperidine ([^{123}I]-FMIP) as a novel single photon emission computed tomography (SPECT) tracer for imaging P-gp at the brain in vivo.

Methods: The tissue distribution and brain uptake as well as the metabolic profile of [^{123}I]-FMIP in wild-type and mdr1a (−/−) mice after pretreatment with physiological saline or cyclosporin A (CsA) (50 mg/kg) was investigated. The influence of increasing doses CsA on brain uptake of [^{123}I]-FMIP was explored. μSPECT images of mice brain after injection of 11.1 MBq [^{123}I]-FMIP were obtained for different treatment strategies thereby using the Milabs U-SPECT-II.

Results: Modulation of P-gp with CsA (50 mg/kg) as well as *mdr1a* gene depletion resulted in significant increase in cerebral uptake of [^{123}I]-FMIP with only minor effect on blood activity. [^{123}I]-FMIP is relative stable in vivo with >80% intact [^{123}I]-FMIP in brain at 60 min p.i. in the different treatment regiments. A dose-dependent sigmoidal increase in brain uptake of [^{123}I]-FMIP with increasing doses of CsA was observed. In vivo region of interest-based SPECT measurements correlated well with the observations of the biodistribution studies.

Conclusions: These findings indicate that [^{123}I]-FMIP can be applied to assess the efficacy of newly developed P-gp modulators. It is also suggested that [^{123}I]-FMIP is a promising SPECT tracer for imaging P-gp at the blood-brain barrier.

Keywords: P-gp; SPECT; Brain; [^{123}I]-4-(2-(bis(4-fluorophenyl)methoxy)ethyl)-1-(4-iodobenzyl)piperidine

1. Introduction

The best known and probably most important energy-dependent drug efflux transporter, P-glycoprotein (P-gp), is a member of the adenosine triphosphate-binding cassette transporters. The human P-gp consists of 1280 amino acids and weighs 170 kDA. It contains two nonidentical homologous parts joined together by a short linker region [1–4].

P-gp is expressed in several normal tissues including the liver, kidneys, intestines, testes and brain. In brain, P-gp is localized at the luminal membrane of endothelial cells [5–8]. It contributes to the efflux of a wide range of xenobiotics at the BBB. Hence, P-gp can play a major role in drug resistance to anti-epileptics [9–11], anti-HIV drugs [12], antidepressants [13] and others [14–18]. Changes or abnormalities in P-gp expression and function are also involved in the etiology and pathogenesis of several neurological diseases [19–23]. A decreased P-gp function, for example, diminishes the clearance of amyloid plaques,

* Corresponding author. Tel.: +32 9 264 8066; fax: +32 9 264 8071.
E-mail address: filipx.devos@ugent.be (F. De Vos).

0969-8051/$ – see front matter © 2010 Published by Elsevier Inc.
doi:10.1016/j.nucmedbio.2009.10.006

increasing the vulnerability to Alzheimer disease [24]. Apart from its role in the central nervous system, P-gp is overexpressed in tumors and therefore implicated in the resistance to chemotherapeutics and involved in the pathogenesis of cancer [25,26].

Modulation of P-gp activity with nontoxic compounds might increase the pharmacological effects of certain anticancer drugs and other P-gp substrates and is therefore potentially of clinical importance. Imaging of P-gp function and expression with positron emission tomography (PET) or single photon emission computed tomography (SPECT) can be of great significance in the development and evaluation of the efficacy of new P-gp modulators. Noninvasive monitoring of P-gp can also be applied to elucidate the role of P-gp in several human diseases. Several tracers have already been evaluated for P-gp modulation among which [^{11}C]verapamil [27–29], [^{11}C]colchicine [30], [^{11}C]daunorubicin [27], [^{18}F]paclitaxel [31], [^{11}C]carvedilol [32], [^{64}Cu]complexes [33,34], [^{11}C]loperamide and [^{11}C]*N*-desmethyl-loperamide [35,36] for PET. [^{11}C]Verapamil is the best studied PET tracer for measuring P-gp function and has already been applied in humans [37–39]. [^{99m}Tc]sestamibi [40,41] and [^{99m}Tc]tetrofosmin [42] are SPECT radiotracers used for measuring P-gp function. However, [^{99m}Tc]sestamibi and [^{99m}Tc]tetrofosmin are not only substrates for P-gp but are also involved in multidrug resistance-associated protein mediated efflux and are not suitable for P-gp imaging in the brain [40–44]. To date, no iodinated SPECT ligands for P-gp imaging were published. The use of SPECT tracers is, in contrast to PET ligands, not limited to nuclear medicine departments with an one-site cyclotron. Furthermore, ^{123}I is an attractive radionuclide for SPECT imaging because it emits abundant 159 keV photons and has a half life of 13.3 h, which are ideal for imaging slower kinetics.

This study describes the *in vivo* evaluation of the first reported iodinated P-gp tracer, [^{123}I]-4-(2-(bis(4-fluorophenyl)methoxy)ethyl)-1-(4-iodobenzyl)piperidine ([^{123}I]-FMIP). [^{123}I]-FMIP (Fig. 1) was originally designed as a tracer for the dopamine transporter but did not display the anticipated in vivo behaviour. Brain uptake was only minor which lead us to the hypothesis that [^{123}I]-FMIP might be a substrate for the P-gp transporter [45]. Therefore, we investigated the influence of P-gp blocking with cyclosporin A (CsA) on the biodistribution and brain penetration of [^{123}I]-FMIP, as well as, the biodistribution of [^{123}I]-FMIP in P-gp knock-out mice. The metabolic profile of [^{123}I]-FMIP was determined and the influence of CsA pretreatment and *mdr1a* gene depletion on the metabolism of [^{123}I]-FMIP was investigated. A dose-response study was performed to assess the impact of increasing CsA dose on the brain uptake of [^{123}I]-FMIP. Finally, a multipinhole μSPECT study of the brain uptake of [^{123}I]-FMIP was performed using the Milabs U-SPECT-II in wild type mice (with and without CsA administration) and in P-gp knockout mice [mdr1a (−/−) mice].

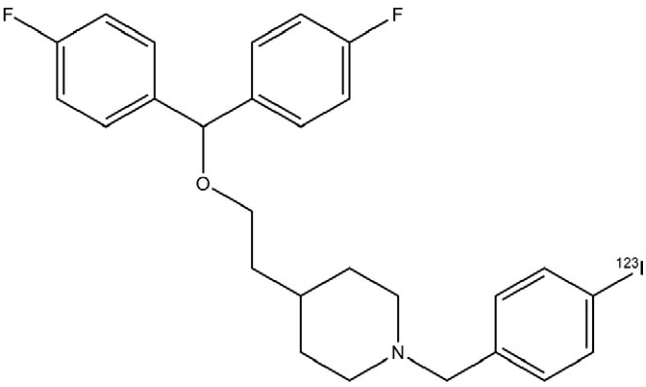

Fig. 1. Structure of [^{123}I]-FMIP.

2. Materials and methods

2.1. General

Cyclosporin A (Sandimmune) was obtained from Novartis Pharma (250 mg/5 ml, Vilvoorde, Belgium). All solvents and chemicals were purchased from Sigma-Aldrich (Bornem, Belgium). No-carrier-added [^{123}I]NaI (in 0.05 M NaOH) was purchased from GE Healthcare (Cygne, The Netherlands).

Radioactivity was counted with an automated gamma-ray spectrometer equipped with five 1x1 inch NaI(Tl) crystals (Cobra Autogamma, Packard Canberra).

Male wild-type mice (FVB or NMRI strain) were purchased from Bioservices. The male mdr1a (−/−) mice (developed with FVB strain), also referred to as P-gp knock-out mice, were obtained from Taconic.

All animal studies were conducted following the principles of laboratory animal care and the Belgian Law on the protection of animals. The performed experiments are approved by the local Ethical Committee of Ghent University (ECP 09/07 and ECP 07/28).

Statistical analysis was performed using the unpaired, one-sided Student's *t* test. $P<.05$ is considered as significant.

2.2. Radiochemistry

[^{123}I]-FMIP was prepared in a 40±10% radiochemical yield, as previously described [36]. The specific activity was >667 GBq/μmol and radiochemical purity appeared to be higher then 98% [36]. [^{123}I]-FMIP was formulated in a 8:92 (v:v) ethanol:saline solution for in vivo studies.

2.3. Biodistribution studies

The biodistribution of [^{123}I]-FMIP was studied in male FVB mice and mdr1a (−/−) mice of 5–7 weeks old weighing 20–25 g. The FVB and mdr1a (−/−) mice were divided into two groups. One group received an injection of CsA in a 50-mg/kg dose. The second group received the same volume physiological saline as control. After 30 min, approximately

185 kBq (5 μCi) [^{123}I]-FMIP was injected intravenously and mice (n=3 for each group and each time point) were sacrificed at 1, 10, 30, 60 and 180 min after [^{123}I]-FMIP injection. Organs and tissues were removed and weighed. All organs were rinsed with water prior to weighing and counting. For calculation of the injected dose, five aliquots of the injection solution were weighed and counted for activity. The radioactivity was measured using an automated gamma-counter. Radioactivity concentrations are decay corrected and expressed as percentage of injected dose per gram of tissue±S.D. (% ID/g tissue±S.D.).

2.4. Plasma protein binding

Plasma protein binding was determined according to literature procedures [37,38]. In brief, a known amount of radiotracer [37 kBq (1 μCi)] was added to 500 μl mouse plasma and incubated for 10 min at room temperature. Three aliquots (30 μl) of spiked plasma were counted for radioactivity. The remaining plasma was transferred onto a Centrifree device with a nominal molecular weight limit of 30 kDa (Amicon, Millipore) and centrifuged for 15 min at 4000×g. The top part of the Centrifree tube was discarded, and three aliquots (30 μl) of the solution remaining in the bottom cup (unbound fraction) were counted for radioactivity. The plasma protein binding was determined by calculating the free fraction as the ratio of the counts of filtered aliquot to the counts of noncentrifuged aliquot.

2.5. Metabolite analysis

The metabolic pattern of [^{123}I]-FMIP and the influence of CsA pretreatment, as well as the influence of depletion of the *mdr1a* gene were investigated.

Male FVB and mdr1a (−/−) mice (approximately 6 weeks old and 25 g) were injected with CsA (50 mg/kg) or physiological saline 30 min prior to the administration of 1.85–3.7 MBq (50–100 μCi) [^{123}I]-FMIP. At 10 (n=3) and 60 min (n=3) p.i., the mice were sacrificed and blood and brain were removed. Blood was collected into a vacutest tube containing 3.6 mg K_3EDTA and was centrifuged at 4000×g for 6 min to separate plasma; 200 μl plasma was mixed with 800 μl acetonitrile, vortexed briefly and centrifuged at 3500×g for 3 min. Brain tissues were homogenized, mixed with 1.5 ml acetonitrile, vortexed and centrifuged at 3500×g for 3 min. Pellet and supernatant were separated and counted for radioactivity using the gamma counter. An aliquot (500 μl) of the supernatant obtained from the plasma and brain homogenates were subjected to reversed-phase high-performance liquid chromatography (HPLC) analysis (Alltima C_{18} 250 mm×10 mm, 10 μm) using 91:9:0.1 (v:v) methanol: H_2O:NH_4OH as solvent system at a flow rate of 6 mL/min. The eluate was collected in 0.5 min fractions and their radioactivity was measured.

To determine recovery capabilities of [^{123}I]-FMIP, as well as the stability of the radiotracer during the workup, control experiments (n=3) were done using plasma and brain spiked with 37 kBq (1 μCi) authentic [^{123}I]-FMIP. Sample workup was identical as described above. Results are expressed as percentages of the total activity±S.D.

2.6. Dose response study with Cyclosporin A

Male NMRI mice weighing 22–28 g were injected in the tail vein with increasing amounts of CsA. The dosages used were 10, 20, 25, 30, 40, 50 and 60 mg/kg. [^{123}I]-FMIP [185 kBq (5 μCi)] was administrated intravenously 30 min after CsA injection. The mice (n=3 for each dosage) were sacrificed at 40 min p.i. of [^{123}I]-FMIP. Three control animals receiving physiological saline were subjected to the same protocol. Blood and organs were removed, weighed and counted for radioactivity in an automated gamma counter. All organs were rinsed with water prior to weighing and counting. For calculation of the injected dose, five aliquots of the injection solution were weighed and counted for activity. Decay-corrected results are expressed as % ID/g tissue±S.D.

Using Graphpad, a dose-response curve was fitted by a sigmoidal curve that is described by the four parameter logistic equation:

$$y = y_0 + (y_{max} - y_0) / \left(1 + 10^{[(log\ EC_{50} - x)*n]}\right)$$

where y is the response, x is the logarithm of concentration, EC_{50} is the half-maximum effect dose and n is the Hill coefficient.

2.7. Multi-pinhole μSPECT imaging

Mice were divided into three groups (n=3 for each group). The first group, Test Group A, was injected with 50 mg/kg CsA, 30 min before tracer injection, whereas the control group and Test Group B received physiological saline. In the control group and Test Group A, FVB mice were used. Test Group B, on the other hand, consisted of mdr1a (−/−) mice.

Dynamic scanning in 12 frames of 5 minutes was performed at 30 min p.i. of [^{123}I]-FMIP using the Milabs U-SPECT-II. This μSPECT scanner is equipped with collimators consisting of a tungsten cylinder with five rings of 15 pinhole apertures of 0.6 mm diameter. All pinholes focused on a single volume in the center of the tube. For imaging mice brain, the animal bed was translated in three dimensions using an XYZ stage into 12 different bed positions. This aforementioned combination enabled a multiple-position acquisition and dynamic imaging at a time scale of a few minutes. Mice were injected with 11.1 MBq (300 μCi) [^{123}I]-FMIP and anesthetized throughout the μSPECT scan by inhalation of 1.5% isoflurane. The 20% photopeak was centered at 159 keV and a double 10% energy window correction at 135 and 190 keV was applied. The data were reconstructed on 0.375 voxels by three iterations of 16 OSEM subsets. The images were postfiltered by a Gaussian of 1.125 mm kernel width and color scales were normalized. A cylindrical brain region of interest (ROI)

of 25 mm^3 (4-mm diameter and 2-mm height) was drawn on the brain for further analysis.

2.8. Statistical analysis

Differences in tissue uptake of [^{123}I]-FMIP between the two treatment regiments and wild-type and mdr1a (−/−) mice were analysed using the one-sided, unpaired Student's *t* test. Only *P* values <.05 are considered significant.

3. Results

3.1. Biodistribution studies of [^{123}I]-FMIP in FVB and mdr1a (−/−) mice with and without CsA

Fig. 2 shows the tissue distribution of radioactivity uptake after intravenous injection of 185 kBq (5 μCi) [^{123}I]-FMIP in wild-type and mdr1a knockout mice with physiological saline or CsA pretreatment.

In the biodistribution study in wild-type mice without CsA pretreatment, the brain uptake was low at each time point investigated (1.08±0.60% ID/g at 1 min p.i. and 0.41±0.24% ID/g at 60 min p.i.). Although [^{123}I]-FMIP was rapidly cleared out of the blood, blood activity remained higher than brain activity at all time points (Fig. 3). At 60 min p.i., the highest tracer uptake was observed in liver with 36.38±18.12% ID/g. Other peripheral organs with high tracer uptake at 60 min p.i. were lungs (9.74±6.01% ID/g), kidneys (7.23±2.46% ID/g) and spleen (7.34±4.90% ID/g).

Modulation of P-gp with intravenously administrated CsA at 50 mg/kg resulted in significant changes in cerebral uptake of [^{123}I]-FMIP (Fig. 3). Brain uptake raised 2.6–5.1-fold compared to mice without CsA pretreatment. At 10 min p.i., the highest increase was observed (5.09±1.48). In addition, in blood and other tissues, no significant modulating effects on [^{123}I]-FMIP concentration were observed after administration of CsA (Fig. 2).

In mdr1a (−/−) mice, [^{123}I]-FMIP content was increased 2.9–5.0 fold in the brain compared to wild-type mice with the highest increase at 30 min p.i. (4.95±0.81) (Fig. 3). In contrast, no significant differences in [^{123}I]-FMIP levels in plasma and other tissues were measured between the two types of mice (Fig. 2). Although liver, kidneys and intestines tended to a lower radioactivity uptake in the mdr1a (−/−) mice, this decrease was not significant.

Pretreatment of mdr1a (−/−) mice with CsA had no additional significant effect on brain activity except at the earliest time point. At 1 min p.i., not only brain but also blood uptake was increased resulting in similar brain/blood ratio. In addition, heart and lung uptake were significantly increased. At 60 and 180 min p.i., a significant increase in intestinal uptake was observed after CsA pretreatment.

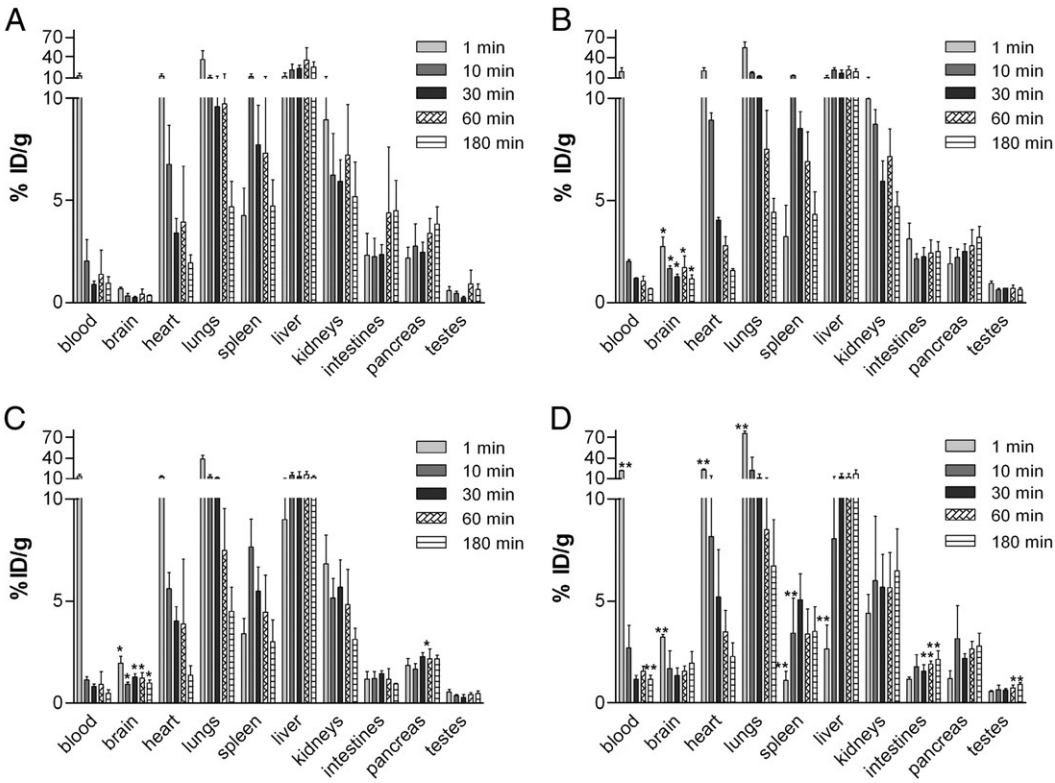

Fig. 2. Tissue distribution at different time points p.i. of 185 kBq (5 μCi) [^{123}I]-FMIP in wild-type and mdr1a knock-out mice with saline or CsA pre-administration. Tracer uptake is expressed as % ID/g tissue±S.D., averaged (*n*=3) and decay-corrected. (A) Pretreatment with saline in wild-type mice. (B) Pretreatment with CsA in wild-type mice. (C) Pretreatment with saline in mdr1a (−/−) mice. (D) Pretreatment with CsA in mdr1a (−/−) mice. **P*<.05 (Student's *t* test) compared to Group A; ***P*<.05 (Student's *t* test) compared to Group C.

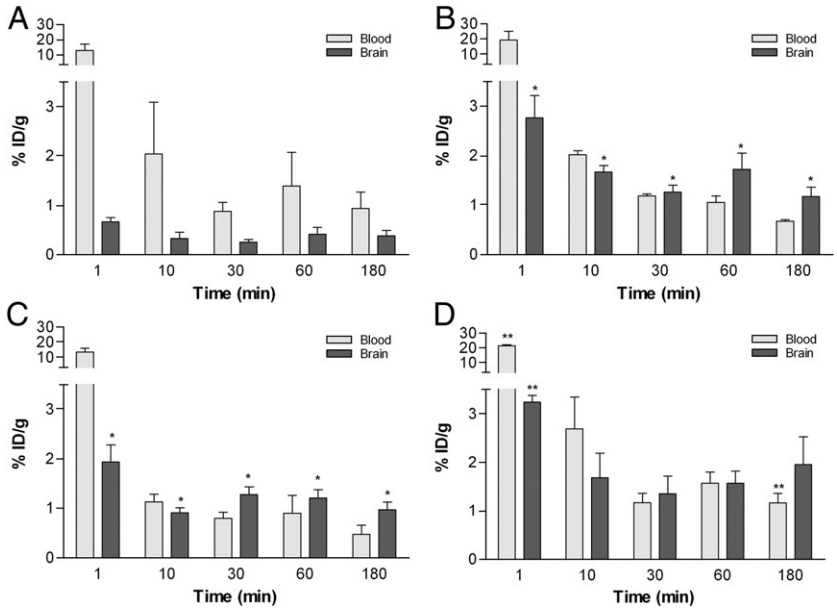

Fig. 3. Effect of CsA and mdr1a depletion on the brain and blood distribution of [^{123}I]-FMIP. Tracer uptake is expressed as % ID/g tissue±S.D., averaged (n=3) and decay-corrected. (A) Pretreatment with saline in wild-type mice. (B) Pretreatment with CsA in wild-type mice. (C) Pretreatment with saline in mdr1a (−/−) mice. (D) Pretreatment with CsA in mdr1a (−/−) mice. *P<.05 (Student's t test) compared to group A; **P<.05 (Student's t test) compared to Group C.

3.2. Plasma protein binding and metabolite analysis

Determination of plasma protein binding revealed that 96±2% of [^{123}I]-FMIP was bound to plasma proteins. Control experiments with spiked plasma and brain revealed an extraction efficiency of 76±4% for plasma and 82±7% for brain samples. The extraction efficiencies obtained during the metabolite experiment were in the same magnitude for the two time points. HPLC analysis of the spiked samples showed that all extracted radioactivity complies with [^{123}I]-FMIP.

Metabolite analysis of plasma in wild-type mice demonstrated that at 10 min p.i. 70±6% and at 60 min p.i. 54±8% of intact [^{123}I]-FMIP is remaining (Fig. 4). Degradation products in plasma were $^{123}I^{-}$ (13±1% at 10 min p.i. and 39±4% at 60 min p.i.) and a lipophilic metabolite with a retention time of 9 min that eluates just before the parent compound (17±7% at 10 min p.i. and 8±4% at 60 min p.i.). In brain, percentages of intact [^{123}I]-FMIP were 86±2% at 10 min p.i. and 85±3% at 60 min p.i. (Fig. 4). The detected metabolites were free iodine (8±2% at 10 min p.i. and 12±4% at 60 min p.i.) and a hydrophilic degradation product with a retention time of 5.5 min (5±1% at 10 min p.i. and 4±1% at 60 min p.i.).

Pretreatment with CsA resulted in less degradation in the brain with 94±3% and 93±5% intact [^{123}I]-FMIP at 10 min

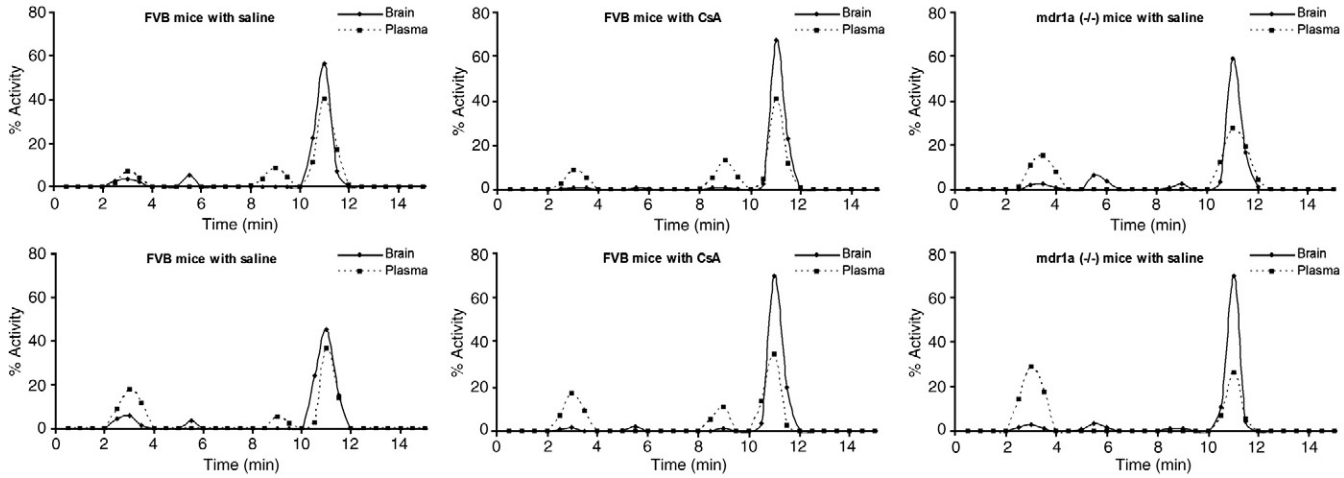

Fig. 4. Metabolite chromatogram at 10 min p.i. (A) and 60 min p.i. (B) of 1.85–3.7 MBq (50–100 μCi) [^{123}I]-FMIP in FVB and mdr1a (−/−) mice after saline and CsA pretreatment. Values are expressed as percentage of total activity and are the mean of three experiments.

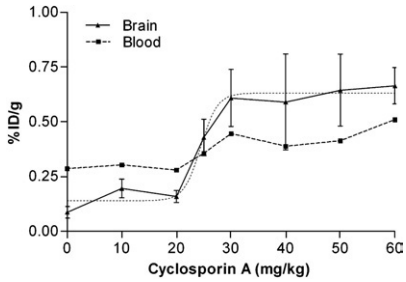

Fig. 5. Effects of various doses CsA on brain uptake and blood concentration of [^{123}I]-FMIP. Tracer uptake is expressed as % ID/g tissue±S.D., averaged (n=3) and decay-corrected.

and 60 min p.i., respectively. The formation of an extra metabolization product (2±1% at 10 min p.i. and 1±1% at 60 min p.i.) with the same retention time of that found in plasma was observed. In plasma, pretreatment with CsA caused an increase in metabolism of [^{123}I]-FMIP at 10 min p.i., while at 60 min p.i., the fraction of [^{123}I]-FMIP remained unchanged (Fig. 4).

Depletion of the *mdr1a* gene had no effect on the fraction of radioactivity present as [^{123}I]-FMIP in brain. Just as observed with CsA pretreatment, the same extra metabolization product was found (3±3% at 10 min p.i. and 2±0% at 60 min p.i.). In plasma, on the other hand, a high increase in the fraction of free iodine was observed. At 60 min p.i., $^{123}I^-$ was the only extracted degradation product (Fig. 4).

3.3. Dose Response study with CsA

The effects of increasing doses CsA on the brain uptake and blood concentration of [^{123}I]-FMIP was investigated (Fig. 5). The experiment showed a sigmoid relationship between the concentration of CsA administrated and the uptake of [^{123}I]-FMIP in the brain. The EC_{50} value was 24.48±0.73 mg/kg. With a higher dose of CsA, a higher brain uptake is observed with a stagnation from 30 mg/kg CsA. Between 30 mg/kg (0.61±0.13% ID/g) and 60 mg/kg (0.56±0.23% ID/g) CsA, there was no significant difference in brain uptake. The effect of CsA administration on the brain uptake was significant at each dosage used compared to the control group. Only a minor increase in blood activity was observed after administration of increasing doses of CsA. Blood uptake of radioactivity without CsA

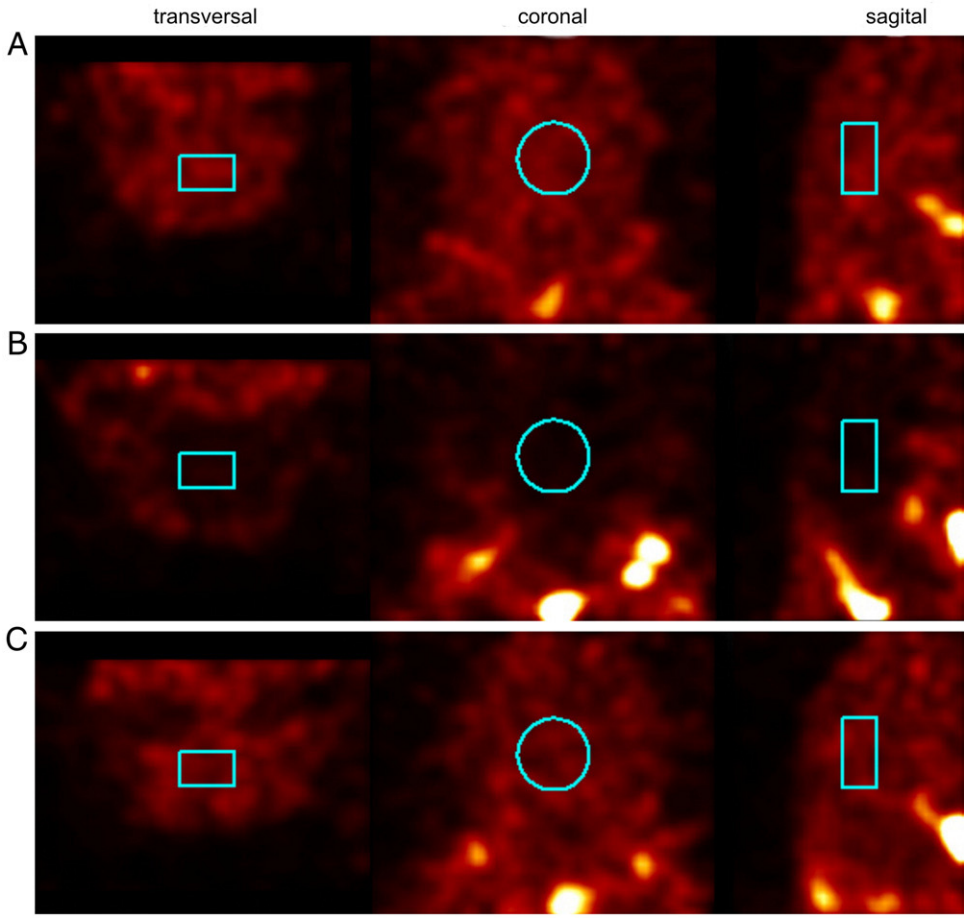

Fig. 6. μSPECT image of mice brain at 60 min p.i. of 11.1 MBq (300 μCi) [^{123}I]-FMIP. ROIs were drawn around the middle of the brain. Mice were anesthetized with isoflurane. (A) pretreatment with CsA (50 mg/kg) 30 min before [^{123}I]-FMIP injection in wild-type mice. (B) Pretreatment with saline 30 min before [^{123}I]-FMIP injection in wild-type mice. (C) Pretreatment with saline 30 min before [^{123}I]-FMIP injection in mdr1a (−/−) mice.

Table 1
Comparison of brain ratios of [123I]-FMIP in biodistribution and μSPECT imaging

	Experiment	30 min p.i.	60 min p.i.
Influence CsA[a]	biodistribution study	4.92±1.94	4.17±2.79
	μSPECT imaging	2.87±0.83	3.04±0.73
Influence gene depletion[b]	biodistribution study	4.95±2.03	2.92±1.85
	μSPECT imaging	2.24±0.35	2.92±0.56

Values are mean of three experiments±S.D., decay-corrected.
[a] Brain uptake in wild-type mice pretreated with CsA/brain uptake in wild-type mice pretreated with saline.
[b] Brain uptake in wild-type mice pretreated with saline/brain uptake in mdr1 (−/−) mice pretreated with saline.

pretreatment was 0.29±0.14% ID/g and increased to 0.51±0.06% ID/g at the highest dose CsA used, but the increase was not significant.

3.4. Small animal SPECT studies

The μSPECT images obtained are shown in Fig. 6. A low homogenous brain uptake was observed after injection of [^{123}I]-FMIP. As seen in Fig. 6, almost no activity was visible on the μSPECT scan. Radioactivity uptake in brain, integrated over the full scan time of 60 min (all 12 frames), was considerably higher after CsA pretreatment as well as in mdr1a (−/−) mice. In the experiment in which CsA had been administered to block P-gp, radioactivity concentration was on average 3.94±0.84 fold higher compared to the baseline experiment. The ratio of brain radioactivity in test group B to that in the control group was about 4.27±1.20 times increased.

The correlation of the biodistribution studies with μSPECT measurements are presented in Table 1. ROIs were evaluated at 30 min p.i. (first 6 frames) and at 60 min p.i. (last six frames) for an exact comparison with the values of the biodistribution studies. The increase in brain uptake after CsA pretreatment and in mdr1a (−/−) mice is slightly higher in biodistribution studies compared to measurements obtained from μSPECT imaging (Table 1).

4. Discussion

P-gp is among other localizations expressed in the blood-brain barrier where it prevents accumulation of certain xenobiotics in the brain by an active transport mechanism. Hence, P-gp can play a significant role in the resistance to central nervous system drugs [9–16]. P-gp has also been associated with several human disorders [17–21]. Noninvasive monitoring of P-gp function can be applied to elucidate the role of P-gp in these human diseases and to evaluate the efficacy of new P-gp modulators. Several tracers have already been evaluated for P-gp imaging but so far, no iodinated SPECT tracer for P-gp has been reported. An iodinated SPECT tracer for P-gp may be especially be important to monitor slower kinetics [46].

The aim of this study was to evaluate the usefulness of [^{123}I]-FMIP for SPECT imaging of the P-gp transporters in the brain. The synthesis and radiosynthesis of [^{123}I]-FMIP are reported elsewhere [36].

The tissue distribution of [^{123}I]-FMIP in wild-type mice without CsA administration was in accordance with that of [^{11}C]verapamil [26] and [^{11}C]*N*-desmethyl-loperamide [29,30]. The lack of brain entrance is consistent with [^{123}I]-FMIP being an avid substrate for P-gp. Intestinal uptake of [^{123}I]-FMIP was low, suggesting mainly urinary and no biliary clearance [47].

CsA is a potent modulator of P-gp in vivo and used in several other studies to assess possible modulation of tracers by P-gp [26,29,39–41]. The biodistribution studies revealed a 2.6–5.1-fold increase in brain uptake after blocking P-gp with CsA. The effect on blood activity was negligible indicating that the increased brain uptake is the result of a decreased tracer efflux and not due to an improved influx to the brain. Additional proof of P-gp involvement was obtained in the study with mdr1a (−/−) mice. In this study, we demonstrated a three- to fivefold increase in brain radioactivity depending on the time point of sacrificing. The use of P-gp knock-out mice did not affect the peripheral tissue distribution. Pretreatment of mdr1a (−/−) mice with CsA caused a significant increase in heart and lung uptake, an effect that is probably caused by the increased blood pool activity and not P-gp mediated. In addition, a significant increase in intestinal uptake was observed at the later time points. This effect could be the cause of a shift in excretion after CsA administration. CsA administration did not affect [^{123}I]-FMIP brain levels in mdr1a (−/−) mice, indicating that [^{123}I]-FMIP is specific towards P-gp [48].

Since P-gp is located in many organs, its blockade might alter the distribution and metabolism of [^{123}I]-FMIP and, thereby, indirectly affect uptake into brain. P-gp blockade with CsA and gene depletion had only little effect on the distribution of radioactivity in body, with exception of the brain. These results confirm that the effect of increased brain uptake was at the blood-brain barrier and not in the periphery. The finding that no significant differences in other organs containing P-gp, like liver and kidneys, were observed corresponds with those reported in other studies [26,42] and can be explained by (1) the unique barrier of the brain, (2) the role of liver and kidneys in excretion and metabolism, (3) up-regulation of mdr1b P-gp in the liver and the kidneys and (4) experimental artefacts (bile ducts are not dissected apart from the liver [49].

The increase in brain uptake observed in the biodistribution study with mdr1a (−/−) mice is lower compared to the increase in brain uptake of [^{11}C]verapamil in mdr1a (−/−) mice [26]. This can be explained by the higher lipophilicity of [^{123}I]-FMIP resulting in strong binding to plasma proteins. It has to be stated that this less pronounced brain accumulation both in P-gp knockout mice and CsA pretreated wild-type mice is not a reflection of the P-gp substrate efficiency, since the potency and affinity of [^{123}I]-

FMIP is proved by the lack op brain accumulation in the wild-type mice and by the results of the dose escalation study [50].

A dose escalation study with increasing concentrations CsA revealed a sigmoidal dose-response relationship between the dose CsA administrated and the brain uptake of [^{123}I]-FMIP. An EC_{50} value of 24.48 mg/kg was obtained. This study demonstrated that the blockade of [^{123}I]-FMIP efflux by P-gp is saturated and complete at a CsA dosage of 30 mg/kg. The dose with maximal tracer uptake and the EC_{50} value are comparable with the values reported for other tracers. [^{11}C]Carvedilol, for example, reached maximum brain uptake at a dosage of 30 mg/kg CsA and did not further increase when mice are pretreated with a higher dose CsA [40]. [^{11}C]verapamil has an EC_{50} value of 22.76 which is comparable with that of [^{123}I]-FMIP, indicating that [^{123}I]-FMIP is an equally potent substrate of P-gp as [^{11}C]verapamil [43]. The differences in the radioactivity uptake between the biodistribution study and the dose escalation study can be explained by the use of a different mouse strain [51].

Determination of plasma protein binding revealed that 96±2% of [^{123}I]-FMIP was bound to plasma proteins. The extraction efficiencies obtained in the metabolite study are high indicating that the binding of [^{123}I]-FMIP to plasma proteins is reversible. No degradation of [^{123}I]-FMIP occurred during the extraction procedure. [^{123}I]-FMIP shows a fairly stable in vivo metabolic profile. One labelled metabolite (retention time=9 min) is probably also a substrate for P-gp as the metabolite only occurs in brain after CsA pretreatment and in mdr1a (−/−) mice. This compound is believed to have a structure close to the parent compound and probably originates from a hydroxylation on a phenyl group or defluorination of a phenyl ring. The fraction of this metabolite however is negligible (<5%). The polar metabolite detected at 5.5 min is possibly the result of *N*-dealkylation. Radioactivity in brain was mainly (>80%) present as intact [^{123}I]-FMIP at the two time points in the three different treatment regimens [52].

Comparison of biodistribution data with *in vivo* ROI-based μSPECT observations showed a good correlation. With mdr1a (−/−) mice, the biodistribution study showed at 60 min p.i. a 2.92±1.85 fold increase in brain uptake of [^{123}I]-FMIP, whereas μSPECT measurements revealed an 2.92±0.56 fold increase. In biodistribution studies, pre-treatment with CsA resulted in 4.17±2.79 higher brain uptake which is in agreement with the 3.04±0.73 increase obtained with μSPECT imaging. Using μSPECT measurements, the obtained standard errors where remarkably lower compared to those of the biodistribution studies. This emphasizes the potential benefits of μSPECT in tracer design. While the brain was visible as a black cavity when only [^{123}I]-FMIP was administrated, CsA administration or the use of mdr1a (−/−) mice improved brain uptake of [^{123}I]-FMIP resulting in a better image of the brain [53].

5. Conclusion

These results indicate that [^{123}I]-FMIP is an avid substrate of P-gp. The dose-escalation study demonstrated that [^{123}I]-FMIP is a potent substrate for P-gp. It is also suggested that [^{123}I]-FMIP is a promising SPECT radiotracer to visualize P-gp function at the blood-brain barrier although further research has to be performed.

References

[1] Ambudkar SV, Kimchi-Sarfaty C, Sauna ZE, Gottesman M. P-glycoprotein: from genomics to mechanism. Oncogene 2003;22: 7468–85.
[2] Bosch I, Croop JM. P-glycoprotein structure and evolutionary homologies. Cytotechnology 1998;27:1–30.
[3] Gottesman MM, Pastan I, Ambudkar S. P-glycoprotein and multidrug resistance. Curr Opin Genet Dev 1996;6:610–7.
[4] Hsu SIH, Lothstein L, Horwitz SB. Differential overexpression of three *mdr* gene family members in multidrugresistance J774.2 mouse cells. Evidence that distinct P-glycoprotein precursors are encoded by unique mdr genes. J Biol Chem 1989;264:12053–62.
[5] Thiebaut F, Tsuruo T, Hamada H, Gottesman MM, Pastan I, Willingham MC. Cellular localization of the multidrug-resistance gene product P-glycoprotein in normal human tissues. Proc Natl Acad Sci U S A 1987;84:7735–8.
[6] Tanigawara Y. Role of P-glycoprotein in drug disposition. Ther Drug Monit 2000;22:137–40.
[7] Schinkel AH, Jonker JW. Mammalian drug efflux transporters of the ATP binding cassette (ABC) family: an overview. Adv Drug Deliv Rev 2003;55:3–29.
[8] Cordon-Cardo C, O'Brien JP, Casals D, Rittman-Grauer L, Biedler JL, Melamed MR, et al. Multidrug-resistance gene (P-glycoprotein) is expressed by endothelial cells at blood-brain barrier sites. Proc Natl Acad Sci USA 1989;86:695–8.
[9] Löscher W, Potschka H. Role of multidrug transporters in pharmacoresistance to antiepileptic drugs. J Pharmacol Exp Ther 2002;301:7–14.
[10] Luna-Tortós C, Fedrowitz M, Löscher W. Several major antiepileptic drugs are substrates for human P-glycoprotein. Neuropharmacology 2008;55:1364–75.
[11] Löscher W. Drug transporters in the epileptic brain. Epilepsia 2007;48: 8–13.
[12] Kim RB, Fromm MF, Wandel C, Leake B, Wood AJJ, Roden DM, et al. The drug transporter P-glycoprotein limits oral absorption and brain entry of HIV-1 protease inhibitors. J Clin Invest 1998;101: 289–94.
[13] Szabo D, Szabo G, Ocsovszki I, Aszalos A, Molnar J. Anti-psychotic drugs reverse multidrug resistance of tumor cell lines and human AML cells ex-vivo. Cancer Lett 1999;139:115–9.
[14] Schinkel AH, Wagenaar E, Mol CAAM, Van Deemter L. P-glycoprotein in the blood-brain barrier of mice influences the brain penetration and pharmacological activity of many drugs. J Clin Invest 1996;97: 2517–24.
[15] Schinkel AH. P-glycoprotein, a gatekeeper in the blood-brain barrier. Adv Drug Deliv Rev 1999;36:179–94.
[16] Linnet K, Ejsing TBA. review on the impact of P-glycoprotein on the penetration of drugs into the brain. Focus on psychotropic drugs. Eur Neuropsychopharmacol 2008;18:157–69.
[17] Löscher W, Potschka H. Drug resistance in brain diseases and the role of drug efflux transporters. Nat Rev Neurosci 2005;6:591–602.
[18] Zhou SF. Structure, function and regulation of P-glycoprotein and its clinical relevance in drug disposition. Xenobiotica 2008;38: 802–32.

[19] Kwan P, Brodie MJ. Potential role of drug transporters in the pathogenesis of medically intractable epilepsy. Epilepsia 2005;46: 224–35.
[20] Turgut G, Bastemir M, Turgut S, Akin F, Kursunluoglu R, Kaptanoglu B. P-gycoprotein polymorphism in hypo- and hyper-thyroidism patients. Mol Biol Rep 2008;35:693–8.
[21] Kortekaas R, Leenders KL, Van Oostrom JCH, Vaalburg W, Bart J, Willemsen ATM, et al. Blood-brain barrier dysfunction in parkinsonian midbrain in vivo. Ann Neurol 2005;57:176–9.
[22] Langford D, Grigorian A, Hurford R, Adame A, Ellis RJ, Hansen L, et al. Altered P-glycoprotein expression in AIDS patients with HIV encephalitis. J Neuropathol Exp Neurol 2004;63:1038–46.
[23] Lam FC, Liu R, Lu P, Shapiro AB, Renoir JM, Sharom FJ, et al. B-amyloid efflux mediated by p-glycoprotein. J Neurochem 2001;76: 1121–8.
[24] Vogelgesang S, Cascorbi I, Schroeder E, Pahnke J, Kroemer HK, Siegmund W, et al. Deposition of Alzheimer's beta-amyloid is inversely correlated with P-glycoprotein expression in the brains of elderly non-demented humans. Pharmacogenetics 2002;12:535–41.
[25] Gottesman MM, Pastan I. Biochemistry of multidrug resistance mediated by the multidrug transporter. Annu Rev Biochem 1993;62: 385–427.
[26] Gottemann MM, Fojo T, Bates SE. Multidrug resistance in cancer: Role of ATP-dependent transporters. Nat Rev Cancer 2002;2:48–58.
[27] Elsinga PH, Franssen EJF, Hendrikse NH, Fluks L, Weemaes AMA, Van Der Graaf WTA, et al. Carbon-11-labeled daunorubicin and verapamil for probing P-glycoprotein in tumors with PET. J Nucl Med 1996;37:1571–5.
[28] Hendrikse NH, Schinkel AH, de Vries EGE, Fluks E, Van Der Graaf WTA, Willemsen ATM, et al. Complete in vivo reversal of P-glycoprotein pump function in the blood-brain barrier visualized with positron emission tomography. Br J Pharmacol 1998;124:1413–8.
[29] Lee YJ, Maeda J, Kusuhara H, Okauchi T, Inaji M, Nagai Y, Obayashi S, et al. In vivo evaluation of P-glycoprotein function at the blood-brain barrier in nonhuman primates using [^{11}C]verapamil. J Pharmacol Exp Ther 2006;316:647–53.
[30] Levchenko A, Mehta BM, Lee JB, Humm JL, Augensen F, Squire O, et al. Evaluation of ^{11}C-colchicine for PET imaging of multiple drug resistance. J Nucl Med 2000;41:493–501.
[31] Kurdziel KA, Kiesewetter DO, Carson RE, Eckelman WC, Herscovitch P. Biodistribution, radiation dose estimates, and in vivo Pgp modulation studies of ^{18}F-paclitaxel in nonhuman primates. J Nucl Med 2003;44:1330–9.
[32] Bart J, Dijkers EC, Wegman TD, de Vries EG, van der Graaf WT, Groen HJ, et al. New positron emission tomography tracer [^{11}C] carvedilol reveals P-glycoprotein modulation kinetics. Br J Pharmacol 2005;145:1045–51.
[33] Lewis JS, Dearling JL, Sosabowski JK, Zweit J, Carnochan P, Kelland LR, et al. Copper bis(diphosphine) complexes: radiopharmaceuticals for the detection of multi-drug resistance in tumours by PET. Eur J Nucl Med 2000;27:638–46.
[34] Packard AB, Kronauge JF, Barbarics E, Kiani S, Treves ST. Synthesis and biodistribution of a lipophilic ^{64}Cu-labeled monocationic copper (II) complex. Nucl Med Biol 2002;29:289–94.
[35] Lazarova N, Zoghbi SS, Hong J, Seneca N, Tuan E, Gladding RL, et al. Synthesis and evaluation of [*N*-methyl-^{11}C]*N*-Desmethyl-loperamide as a new and improved PET radiotracer for imaging P-gp function. J Med Chem 2008;51:6034–43.
[36] Zoghbi SS, Liow JSL, Yasuno F, Hong J, Tuan E, Lazarova N, et al. ^{11}C-Loperamide and its *N*-desmethyl radiometabolite are avid substrates for brain permeability-glycoprotein efflux. J Nucl Med 2008;49:649–56.
[37] Sasongko L, Link JM, Muzi M, Mankoff DA, Yang XD, Collier AC, et al. Imaging P-glycoprotein transport activity at the human blood-brain barrier with positron emission tomography. Clin Pharmacol Ther 2005;77:503–14.
[38] Abrahim A, Luurtsema G, Bauer M, Karch R, Lubberink M, Pataraia E, et al. Peripheral metabolism of (*R*)-[^{11}C]verapamil in epilepsy patients. Eur J Nucl Med Mol Imaging 2007;35:116–23.
[39] Bartels AL, van Berckel BNM, Lubberink M, Luurtsema G, Lammertsma AA, Leenders KL. Blood-brain barrier P-glycoprotein function is not impaired in early Parkinson's disease. Parkinsonism Relat Disord 2008;14:505–8.
[40] Kostakoglu L, Elahi N, Kïratlï P, Ruacan S, Sayek I, Baltalï E, et al. Clinical validation of the influence of P-glycoprotein on technetium-99m-sestamibi uptake in malignant tumors. J Nucl Med 1997;38: 1003–8.
[41] Ballinger JR, Hua HA, Berry BW, Firby P, Boxen I. ^{99m}Tc-sestamibi as an agent for imaging P-glycoprotein-mediated multidrug resistance: in vitro and in vivo studies in a rat breast tumour cell line and its doxorubicin-resistant variant. Nucl Med Commun 1995;16:253–7.
[42] Ballinger JR, Bannerman J, Boxen I, Firby P, Hartman NG, Moore MJ. Technetium-99m-Tetrofosmin as a substrate for P-glycoprotein: in vitro studies in multidrug-resistant breast tumor cells. J Nucl Med 1996;37:1578–82.
[43] Hendrikse NH, Franssen EJF, van der Graaf WTA, Meijer C, Piers DA, Vaalburg W, et al. Tc-99m-sestamibi is a substrate for P-glycoprotein and the multidrug resistance-associated protein. Br J Cancer 1997;77: 353–8.
[44] Barbarics E, Kronauge JF, Cohen D, Davison A, Jones AG, Croop JM. Characterization of P-glycoprotein transport and inhibition in vivo. Cancer Res 1998;58:276–82.
[45] De Bruyne S, Boos TL, wyffels L, Goeman JL, Rice KC, De Vos F. Synthesis, radiosynthesis and *in vivo* evaluation of [^{123}I]-4-(2-(bis(4-fluorophenyl)methoxy)ethyl)-1-(4-iodobenzyl)piperidine as a selective tracer for imaging the dopamine transporter. J Label Compd Radiopharm 2009;52:304–11.
[46] Gandelman MS, Baldwin RM, Zoghbi SS, Zea-Ponce Y, Innis RB. Evaluation of ultrafiltration for the free fraction determination of single photon emission computerized tomography (SPECT) radiotracers: β-CIT, IBF and iomazenil. J Pharm Sci 1994;83: 1014–9.
[47] Fowler JS, Kroll C, Ferrieri R, Alexoff D, Logan J, Dewey SL, et al. PET studies of *d*- methamphetamine pharmacokinetics in primates: comparison with *l*-methamphetamine and (-)-cocaine. J Nucl Med 2007;48:1724–32.
[48] De Vries EFJ, Doorduin J, Vellinga NAR, Van Waarde A, Dierckx RA, Klein HC. Can celecoxib affect P-glycoprotein-mediated drug efflux? A microPET study. Nucl Med Biol 2008;35:459–66.
[49] Elsinga PH, Hendrikse NH, Bart J, Van Waarde A, Vaalburg W. Positron emission tomography studies on binding of central nervous system drugs and P-glycoprotein function in the rodent brain. Mol Imaging Biol 2005;7:37–44.
[50] Syvanen S, Blomquist G, Sprycha M, Hoglund AU, Roman M, Eriksson O, et al. Duration and degree of cyclosporin induced P-glycoprotein inhibition in the rat blood-brain barrier can be studied with PET. Neuroimage 2006;32:1134–41.
[51] Luurtsema G, Molthoff CFM, Windhorst JW, Smit H, Keizer R, Boellaard AA, et al. (R)- and (S)-[^{11}C]Verapamil as PET-tracers for measuring P-glycoprotein function: *in vitro* and *in vivo* evaluation. Nucl Med Biol 2003;30:747–51.
[52] Bart J, Willemsen ATM, Groen HJM, Van Der Graaf WTA, Wegman TD, Vaalburg W, et al. Quantitative assessment of P-glycoprotein function in the rat blood-brain barrier by distribution volume of [^{11}C] Verapamil measured with PET. Neuroimage 2003;20:1775–82.
[53] Piwnica-Worms D, Kesarwala AH, Pichler A, Prior JL, Sharma V. Single photon emission computed tomography and positron emission tomography imaging of multi-drug resistant P-glycoprotein–Monitoring a transport activity important in cancer, blood-brain barrier function and Alzheimer's disease. Neuroimaging Clin N Am 2006; 16:575–89.